

Branched Amphipathic Peptide Capsules: Different Ratios of the Two Constituent Peptides Direct Distinct Bilayer Structures, Sizes, and DNA Transfection Efficiency

Sheila de M. Barros,^{†,‡} L. Adriana Avila,[§] Susan K. Whitaker,[†] Kayla E. Wilkinson,[†] Pinakin Sukthakar,^{||} Eduardo I. C. Beltrão,[‡] and John M. Tomich^{*,†} 

[†]Department of Biochemistry and Molecular Biophysics, Kansas State University, Manhattan, Kansas 66506, United States

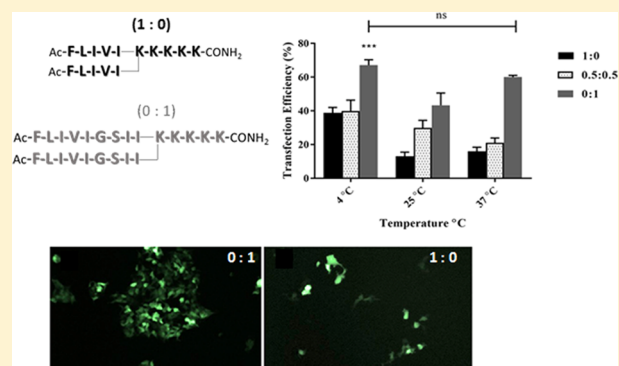
[‡]Department of Biochemistry, Federal University of Pernambuco-UFPE, Recife, Pernambuco 50670-901, Brazil

[§]Department of Chemistry and Biochemistry, Auburn University, Auburn, Alabama 36849, United States

^{||}Department of Molecular Biosciences, University of Kansas, Lawrence, Kansas 66045, United States

Supporting Information

ABSTRACT: Branched amphipathic peptide capsules (BAPCs) are biologically derived, bilayer delimited, nanovesicles capable of being coated by or encapsulating a wide variety of solutes. The vesicles and their cargos are readily taken up by cells and become localized in the perinuclear region of cells. When BAPCs are mixed with DNA, the BAPCs act as cationic nucleation centers around which DNA winds. The BAPCs-DNA nanoparticles are capable of delivering plasmid DNA in vivo and in vitro yielding high transfection rates and minimal cytotoxicity. BAPCs share several biophysical properties with lipid vesicles. They are however considerably more stable—resisting disruption in the presence of chaotropes such as urea and guanidinium chloride, anionic detergents, proteases, and elevated temperature (~95 °C). To date, all of our published results have utilized BAPCs that are composed of equimolar concentrations of the two branched sequences (Ac-FLIVI)₂-K-K₄-CO-NH₂ and (Ac-FLIVIGSII)₂-K-K₄-CO-NH₂. The mixture of sizes was utilized to relieve potential curvature strain in the spherical capsule. In this article, different molar ratios of the two peptides were studied to test whether alternate ratios produced BAPCs with different biological and biophysical properties. Additionally, preparation (annealing) temperature was included as a second variable.



INTRODUCTION

Self-assembling polymeric vesicles have shown promise as gene and drug delivery systems. Vesicles prepared from different oligomers can be generated from a variety of self-assembling molecules^{1–7} with amphiphilic block copolymers being among the most widely studied. The amphiphilic blocks can be synthetic, natural, or a mixture of both. When a peptide comprises one of the segments, the resulting assemblies are termed peptide vesicles or peptosomes. However, few peptide vesicles have been reported in the literature compared to the numerous synthetic polymers capable of self-assembling into vesicles. Vauthey et al.⁸ described a short peptide termed surfactant-like peptide that assembled into nanotubes and nanovesicles. Matsuura et al.^{9,10} reported an artificial C3-symmetric peptide conjugates, trigonal (FKFE)₂, capable of self-assembly into viral-sized peptide nanospheres in water. Van Hell et al.¹¹ showed the self-assembly of an amphiphilic oligopeptide SA2 into nanosized vesicles. More recently, aromatic dipeptides,^{12,13} dipeptides containing a C-terminal

glutamic acid residue,¹⁴ and a tripeptide¹⁵ have been reported to self-assemble into nanovesicles.

Our contribution in this area is branched amphipathic peptide capsules (BAPCs). They are formed through the spontaneous supramolecular assembly of the two peptides (Ac-FLIVI)₂-K-K₄-CO-NH₂ and (Ac-FLIVIGSII)₂-K-K₄-CO-NH₂ in water. We have introduced the term “capsule” in an effort to avoid confusion between our peptidic nanospheres and traditional lipid vesicles. A history detailing the origins of the BAPCs is described in a recent review.¹⁶ Previous studies that included transmission electron microscopy (TEM) and computational simulations indicated that the hollow capsules are bound by a peptide bilayer.¹⁷ The peptides are mixed as helical monomers in the absence of water, dried, and then hydrated to start the annealing process. BAPCs formation is observed after 30 min with nascent capsules assembling into

Received: March 16, 2017

Revised: June 14, 2017

Published: June 27, 2017

sizes ranging from 20 to 30 nm in diameter.¹⁷ If the peptides are assembled at 25 °C, the nascent capsules undergo fusion and within a few hours form heterogeneous spherical structures that ranged in size (50–200 nm).¹⁸ It was observed that BAPCs formed at 25 °C and then moved to 4 °C for as little as 1 h blocked fusion even when they were returned to elevated temperatures (up to 80 °C). BAPCs prepared at either 4 or 37 °C do not undergo fusion and retain the size of the nascent capsules. Sukthankar et al.¹⁸ examined the temperature dependence on the secondary structure, size, and encapsulation efficiency of BAPCs. The peptides present in the BAPCs adopted different conformations: with 4 °C BAPCs showing mostly random structure, 25 °C BAPCs displaying a mixture of random and beta-structure, and the 37 °C ones being mostly in beta.

Peptide vesicles capable of delivering nucleic acids into cells are also relatively rare. To the best of our knowledge, only two research groups had reported the use of peptide vesicles for gene delivery. Li and co-workers¹⁹ described cationic dipeptides (H-Phe-Phe-NH₂-HCl) that self-assemble into nanotubes and rearrange to form vesicles upon dilution. These vesicles were able to deliver small oligos into cells in culture. Our group demonstrated the ability of BAPCs to deliver plasmid DNA (pDNA) in vivo and in vitro.^{20,21} In vitro, BAPCs associated with DNA were capable of delivering plasmid DNA with transfection rates ~55% and minimal cytotoxicity.²¹ In vivo, BAPCs were capable of delivering a vaccine DNA encoding the E7 oncoprotein of HPV-16 (pgDE7) in mice. Mice immunized with pgDE7-BAPC nanocapsules complexes constrained tumor growth up to one month after transplantation of tumor cells without significant toxic effects.²¹ TEM and AFM analysis showed that BAPCs can act as cationic nucleation centers around which DNA winds generating peptide–DNA complexes with a size ranging from 50 to 100 nm.²¹

All of these published studies utilized a 1:1 ratio of the two peptides (Ac-FLIVI)₂-K-K₄-CO-NH₂ and (Ac-FLIVIGSII)₂-K-K₄-CO-NH₂ (Figure 1). This ratio was chosen arbitrarily to



Figure 1. Branched amphipathic peptide capsule (BAPC) forming sequences. The peptides are described in the text as (Ac-FLIVI)₂-K-K₄-CO-NH₂ and (Ac-FLIVIGSII)₂-K-K₄-CO-NH₂, respectively.

allow enough of the smaller peptide to line the inner leaflet with the larger sequence making up the outer leaflet of the assembled bilayer to compensate for any strain due to curvature. In this report we prepared BAPCs where the ratio of the two peptides and the annealing temperatures were modified with an eye toward examining how these variables affected the physical properties and gene delivery efficacies (in vitro) of the capsules. BAPCs were prepared with the following (Ac-FLIVI)₂-K-K₄-CO-NH₂:(Ac-FLIVIGSII)₂-K-K₄-CO-NH₂ ratios –1:0, 0.8:0.2, 0.5:0.5, 0.2:0.8, and 0:1. Also, capsules were annealed at 4, 25, and 37 °C. BAPCs prepared at 4 °C showed the highest efficiency in encapsulating the fluorescent dye Eosin Y and those prepared using just (Ac-FLIVIGSII)₂-K-K₄-CO-NH₂ showed the maximal transfection rates. These results suggest that equimolar concentrations of BAPCs are not

essential for encapsulating solutes and delivering complexed DNA into living cells.

MATERIALS AND METHODS

Peptide Synthesis. Peptides were synthesized by solid phase peptide chemistry on 4-(2,4-dimethoxyphenyl-Fmoc-aminomethyl)-phenoxyacetyl-norleucyl-cross-linked ethoxylate acrylate resin²² (Peptides International Inc.; Louisville, KY) on a 0.1 mmol scale using Fmoc (N-(9-fluorenyl) methoxycarbonyl)/*tert*-butyl chemistry on an ABI Model 431 peptide synthesizer (Applied Biosystems; Foster City, CA) with modified cycles and resin with reduced substitutions. The Fmoc L-amino acids were obtained from Anaspec, Inc. (Fremont, CA). The branch point was introduced by incorporating N^{α,ε} di-Fmoc-L-lysine in the fifth position from the C-terminus. Deprotection of this moiety leads to the generation of two reactive amino sites, thereby generating the bifurcated peptide branch point. This enables the addition two predominantly hydrophobic N-terminal tail segments FLIVI and FLIVIGSII to the common hydrophilic oligo-lysine segment by the stepwise addition of Fmoc amino acids.²³ The N-termini of the peptides were acetylated on the resin using acetic anhydride/*N,N*-diisopropylethylamine/1-hydroxybenzotriazole just prior to cleavage. The peptides were cleaved from the resin using TFA/water (98:2, v/v) for 90 min at RT to generate C-terminal carboxamide. The peptide products were washed 3× with diethyl ether. At this point the two peptides were treated differently. The shorter peptide was redissolved in water prior to lyophilization. The water used throughout this study is first deionized then reverse osmosis treated and finally glass distilled. The larger peptide was dried directly from the ether. The larger peptide has a propensity to form beta-structure in water, leading to the formation of aggregates that persist after lyophilization. Drying directly from ether prevents this. The larger peptide was hydrated just before performing any analysis. The RP-HPLC purified peptides were dried in vacuo and characterized on a Bruker Ultraflex III matrix-assisted laser desorption/ionization time-of-flight mass spectrometer (MALDI TOF/TOF) (Bruker Daltonics, Billerica, MA) using 2,5-dihydroxybenzoic acid matrix (Sigma-Aldrich Corp., St. Louis, MO). The dried peptides were stored at room temperature.

Capsule Formation and Encapsulation. The (Ac-FLIVI)₂-K-K₄-CO-NH₂ and (Ac-FLIVIGSII)₂-K-K₄-CO-NH₂ peptides were dissolved individually in neat 2,2,2-trifluoroethanol. In this solvent the peptides are helical and monomeric, thereby ensuring complete mixing when combined. Concentrations were determined for the stock TFE dissolved samples using the molar extinction coefficient (ϵ) of phenylalanine residues (two per sequence) at 257.5 nm (195 cm⁻¹ M⁻¹).^{24,25} The (Ac-FLIVI)₂-K-K₄-CO-NH₂ and (Ac-FLIVIGSII)₂-K-K₄-CO-NH₂ peptide solutions of known concentration were mixed to yield ratios of 1:0, 0.8:0.2, 0.5:0.5, 0.2:0.8, and 0:1 and then dried in vacuo. BAPCs (50 μ M) samples were prepared by hydrating the dried monomeric mixture of the constituent peptides dried from 100% TFE with aqueous Eosin Y (2.13 mM) or Rhodamine 6G (2 mM and 0.1 mM) and then allowed to assemble for 60 min at 4, 25, or 37 °C. Fluorescence of Eosin Y strongly quenched at this concentration. Rhodamine 6G, which is also self-quenching, was used at two concentrations: one that was quenching (2.0 mM) and the other at a concentration that yielded maximum fluorescence (0.1 mM) (Supporting Information Figure S1). The dye-loaded BAPCs were then washed by centrifugation carried out at 14000g in Amicon ultra-0.5 mL 30 kDa molecular weight cutoff centrifugal cellulose filters (Millipore, Billerica, MA) using a Thermo Electron Legend 14 personal microcentrifuge (Thermo Fisher Scientific Inc., Waltham, MA) to remove nonencapsulated dye. Samples were then subjected to multiple centrifugation cycles starting with a 5 min preincubation with 200 mM Na-TFA salt. The TFA⁻ counterion successfully displaces negatively charged Eosin Y associated with the outer capsule surface.¹⁸ For the second–sixth wash cycles, the dye encapsulated capsules were incubated with just water prior to centrifugation. At the conclusion of the sixth spin, the removable-filter unit was inverted and placed in a fresh tube and spun at 2000g for 5 min to recover the remaining

volume containing the washed capsules. This sample was then diluted to the desired concentration with water.

For studies examining encapsulation efficiency and temperature effects Eosin Y (Sigma-Aldrich Corp., St. Louis, MO) or Rhodamine 6G (Sigma-Aldrich Corp., St. Louis, MO) was present in the hydration solutions at desired concentrations. After BAPC formation in the presence of either dye (60 min) the samples were passed through a 0.2 μm PTFE syringe filter (Millipore Millex FG, Billerica, MA). Fluorescence measurements of the encapsulated contents were carried out by the excitation of Eosin Y at 490 nm and scanning for observed emissions from 495 to 800 nm with a CARY Eclipse fluorescence spectrophotometer (Varian Inc., Palo Alto, CA) (scan rate: 600 nm/min; PMT detector voltage: 600 V; excitation slit: 10 nm; emission slit: 10 nm) using a 0.3 cm path length quartz cuvette. Standard curves examining the concentration and temperature effects on Eosin Y fluorescence were performed and used to correct data obtained for these effects.

For the temperature studies with the different peptide ratios, changes in the fluorescence intensity of the dye Eosin Y were followed as a function of temperature. The dye was used at a concentration that quenches the fluorescence. Any lysis of the BAPCs would result in an increase in fluorescence intensity. For these studies the BAPCs were prepared at 4 °C for at least an hour before washing. The fluorescence was initially measured at 4 °C followed by jumps to 25 °C and then 37 °C followed in some experiments by 10 °C increases up to 95 °C.

Circular Dichroism Experiments. Circular dichroism (CD) experiments were conducted to analyze conformational changes in secondary structures formed by the water-filled 1 mM BAPCs prepared with the different peptide ratios. Data were collected on a Jasco J-815 CD spectrophotometer (Jasco Analytical Instruments, Easton, MD) using a 0.2 mm path length jacketed cylindrical quartz cuvette (Starna Cells Inc., Atascadero, CA). Spectra were scanned from 260 to 190 nm at a scan rate of 50 nm min⁻¹ with 1 nm step intervals. All experimental temperatures were maintained using a heating/cooling fluid circulator (IBM Corp.) connected to the jacketed cuvette. CD spectra were measured in “mdeg” using an average of five scans. The raw data were subtracted from blank at the appropriate temperature and smoothed using a Savitsky–Golay filter^{26,27} using Spectra Analysis software provided by the manufacturer (Jasco Inc., Easton, MD). Peptide concentrations were determined using the absorbance of phenylalanine as previously described.¹⁷

Dynamic Light Scattering and Zeta Potential. Branched amphiphatic peptides with varying ratios of (Ac-FLIVI)₂-K-K₄-CO-NH₂ and (Ac-FLIVIGSII)₂-K-K₄-CO-NH₂ were hydrated at 4 °C to yield BAPCs incorporating a total peptide concentration of 2 mM. These were maintained at 4 °C for 3 h before bringing them to RT prior to analysis. Dynamic light scattering (DLS) and zeta potential (ZP) analysis were performed using a Zetasizer Nano ZS (Malvern Instruments Ltd., Westborough, MA). The accuracy of the instrument was validated using 30 and 90 nm Nanosphere-NIST traceable mean diameter standards (Thermo Fisher Scientific, Waltham, MA).

Cell Culture. HEK-293 cells were kindly donated by Dr. Tao (Auburn University) and maintained as previously described.²¹

Preparation of DNA-BAPCs Nanoparticles. BAPCs (45 μM) were prepared at different ratios of (Ac-FLIVI)₂-K-K₄-CO-NH₂ and (Ac-FLIVIGSII)₂-K-K₄-CO-NH₂ and hydrated at different temperatures (4, 25, and 37 °C). Subsequently, they were mixed with 2.5 μg of pEGFP-N3 (Clontech, Mountain View, CA). The charge ratio (N:P) ratio was 26. The N:P charge ratio for a given complex has been previously defined.²⁰ Solutions were mixed carefully with a pipet and allowed to stand for 10 min at RT before adding CaCl₂, 1.0 mM final concentration. After an additional 30 min incubation period, the solution was added to the cell culture. CaCl₂ alone at this concentration was analyzed and did not to enhance DNA uptake or expression.

In Vitro Plasmid Transfection. For transfection experiments, cells were seeded as previously described;²¹ 24 h later at 60% confluence, all medium was removed from the wells, and 800 μL of Opti-MEM I Reduced Serum Media was added. Next, 200 μL of BAPCs-DNA nanoparticles was added to cells. The BAPCs-DNA

complexes were incubated with cells for 4–6 h at 37 °C/5% CO₂. After the incubation period, media and transfection reagent were removed and replaced with 1 mL of fresh DMEM containing 10% FBS in each well. The cells were returned to the incubator for 48 h. After this incubation period, transfection efficiency was monitored by fluorescence microscopy and quantified by flow cytometry (Accuri C6 Flow Cytometer, Beckon Dickson, San Jose, CA). Ghost Dye Red 780 (Tonbo Biosciences, San Diego, CA) was used to identify and then exclude dead cells from the analysis. Nontransfected cells containing only DNA and CaCl₂ (1 mM) were used as a control. For the positive control, cells were transfected with jetPRIME (PolyPlus, Strasbourg, France) following the manufacturer protocol. Data were analyzed using the FlowJo software V.10.1 (TreeStar, Ashland, OR).

Fluorescence Microscope Images. Images were obtained using an Eclipse Ti2 inverted microscopy system (Nikon, Melville, NY).

RESULTS AND DISCUSSION

Physicochemical and Structural Properties of BAPCs Assembled at Different Temperatures and with Different (Ac-FLIVI)₂-K-K₄-CO-NH₂: (Ac-FLIVIGSII)₂-K-K₄-CO-NH₂ Ratios. All of our published studies were performed using the equimolar ratios of (Ac-FLIVI)₂-K-K₄-CO-NH₂ and (Ac-FLIVIGSII)₂-K-K₄-CO-NH₂. Early in our deliberations on how best to prepare BAPCs, we made the assumption that an equimolar ratio of the large and small sequences would be a reasonable starting point. It was reasoned that if the branched peptides formed vesicle-like structures, including the shorter (Ac-FLIVI)₂-K-K₄-CO-NH₂ sequence with the longer (Ac-FLIVIGSII)₂-K-K₄-CO-NH₂ could ease any strain due to curvature and thereby facilitate assembly. When we examined the actual distribution of the two peptides in the assembled bilayers we observed that the outer leaflet contained both sequences with the larger peptide predominating. Exact ratios were difficult to assess due to the variability involved in the self-assembly process. The ability of this ratio to meet the original design goals left studying the individual peptides as well as all other ratios untested.

In Sukthankar et al.¹⁹ equimolar ratios yielded BAPCs with unusual thermal transitions. Capsules prepared at 25 °C spontaneously fused to form a heterogeneous population of larger spherical structures while those prepared at 4 and 37 °C were uniform spheres with a fixed diameter of 20–30 nm. The secondary structure of the peptides in the assemblies were predominantly random coil or beta-structures for 4° and 37 °C, respectively. The 25 °C peptides were a mixture of the two but transitioned to beta as the capsules grew in size.

In an effort to design BAPCs with new properties, BAPCs (50 μM) were prepared using three different (Ac-FLIVI)₂-K-K₄-CO-NH₂: (Ac-FLIVIGSII)₂-K-K₄-CO-NH₂ ratios (1:0, 0.5:0.5, and 0:1). They were annealed at 4 °C and then tested for thermal stability. The dye Eosin Y was encapsulated at a concentration that shows significant quenching (2.1 mM in water). The washed dye encapsulated BAPCs were ramped rapidly to 25 °C and then heated to 95 °C with 10° increments over a period of 2 h. As depicted in Figure 2, the three different BAPC preparations (1:0 (panel A), 0.5:0.5 (panel B), and 0:1 (panel C) clearly trap the dye during capsule formation and remained intact throughout the experiment as judged by the absence of dye release. At the end of each experiment an equal volume of TFE was added to the sample to yield a 50% TFE solution that causes the capsules to disassemble thereby releasing the dye (dotted line), leading to the expected increase in fluorescence intensity. A 0.5X dilution constant was factored in while graphing the increase in fluorescence intensity due to

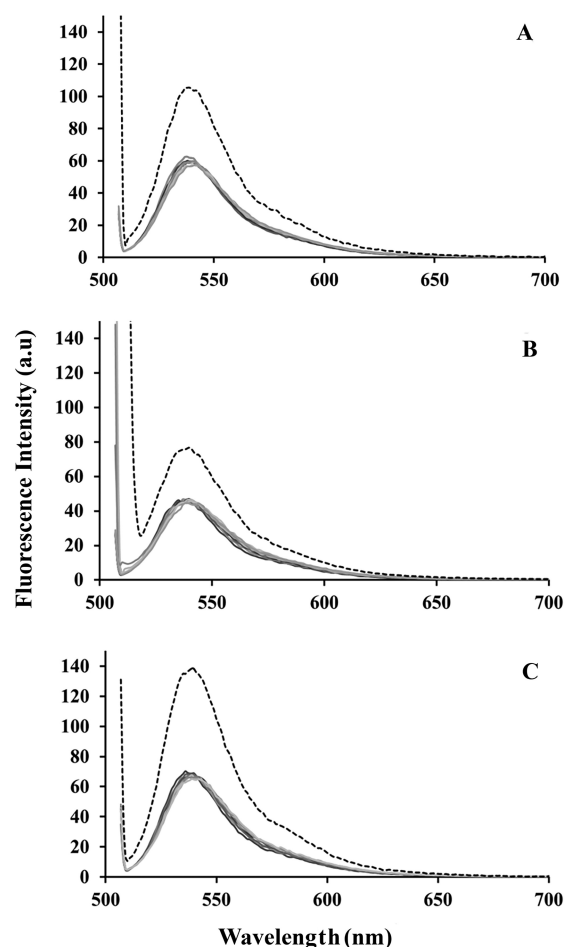


Figure 2. Thermal stability of BAPCs prepared at different peptide ratios. Eosin Y containing BAPCs ($50 \mu\text{M}$) were prepared at 4°C using the ratios 1:0 (A), 0.5:0.5 (B), and 0:1 (C). The temperature was then ramped to 95°C over 2 h. The BAPCs were disassembled in the presence of 50% TFE at the end of the experiment (dashed line).

dye release, to account for the 50% dilution of the sample due to the addition of TFE. This was done for clarity since the released dye curve falls on top of the other spectra. The 50% TFE curve was also corrected for any fluorescence enhancement due to solvent. These results indicate that a mixture of longer and shorter branched peptides is not required for BAPC formation and that encapsulated solutes can be released upon disassembly in 50% TFE solutions.

The peptide and dye concentrations for each ratio were identical; however, the amount of encapsulation was less in the BAPCs prepared with the equimolar peptide ratio. To verify this observation, BAPCs were prepared with the following ratios (1:0, 0.8:0.2, 0.5:0.5, 0.2:0.8, and 0:1). For this experiment the annealing temperatures were included as a second variable. All of the ratios formed BAPCs at the three different temperatures (Figure 3). Previously, Sukthankar et al.¹⁹ showed that encapsulation efficiencies for the equimolar ratio were highest at 4°C and decreased at higher assembly temperatures. This study reveals a similar pattern with the 4°C assemblies showing the highest encapsulation values. Over the conditions tested here is roughly a 4-fold difference in the amount encapsulated comparing the highest loading with the 4°C assembly of just (Ac-FLIVI)-K-K₄-CO-NH₂ compared with the 37°C assembly made using a 0.5:0.5 ratio. Looking within

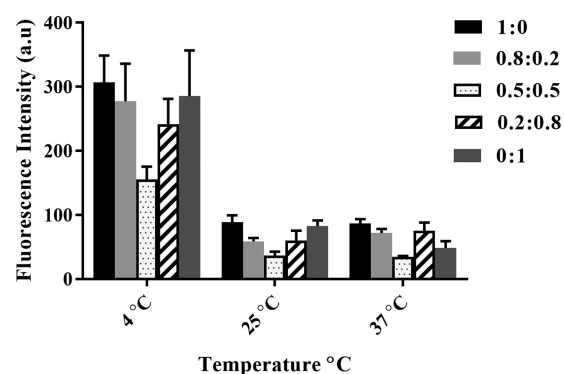


Figure 3. Temperature dependence on dye encapsulation for BAPCs prepared at different peptide ratios for 1 h. Data represent mean values + SEM of three experiments combined.

each temperature grouping the highest values are recorded for the more homogeneous ratios, with the equimolar ratio showing the least amount of trapped solutes during assembly. While the net encapsulation values decreased with increasing temperatures the pattern of increased encapsulation at the more homogeneous ratios was preserved. The trend showing increased encapsulation at the more homogeneous ratios was unexpected. The 0.5:0.5 ratio, which showed the lowest level of dye encapsulation, could be the result of a slower annealing rate or a higher level of precipitation. Examining the Eosin Y encapsulation process carefully we observed tiny colored aggregates in many of the samples. These samples are always filtered using a $0.2 \mu\text{m}$ PTFE syringe filter. The weights of the dried residue left on the filters showed that the equimolar ratio of peptide showed had the highest level of aggregation, double that of a homomeric ratio. A possible explanation for this is discussed in the section that shows the zeta potential for BAPCs formed with the different peptide ratios. This result supports the idea that lower encapsulation is the result of reduced concentrations of the equimolar ratio peptide assembly in the presence of the Eosin Y.

To further test these results, an encapsulation time-course experiment was performed over 24 h at 4°C using Rhodamine 6G (Figure 4). This dye is positively charged and does not interact as strongly with the cationic surface of the capsules. No precipitation was observed when this dye (at quenching concentrations 2.0 mM) was mixed with any of the peptide ratios. The dye was also used at a concentration (0.1 mM) that provides maximum fluorescence. Together, these conditions provide for fluorescence intensities that give the best opportunity to identify any changes in encapsulation over time. The (Ac-FLIVI)₂-K-K₄-CO-NH₂ only (Figure 4A) and (Ac-FLIVIGSII)₂-K-K₄-CO-NH₂ only (Figure 4B) BAPCs along with the 0.5:0.5 ratio (Figure 4C) were tested. With each BAPC ratio, self-assembly at 4°C was essentially complete by 60 min. No significant statistical difference was seen for the times tested. These results supports the idea that the decreased encapsulation efficiency observed for Eosin Y with the equimolar ratio is a consequence of the loss of peptide due to precipitation.

While annealing temperature had no effect on the rates of assembly, earlier studies on BAPCs prepared using an equimolar mixture of (Ac-FLIVI)₂-K-K₄-CO-NH₂ and (Ac-FLIVIGSII)₂-K-K₄-CO-NH₂, the annealing temperature had a profound effect on the secondary structure of the assembled peptides.¹⁸ As stated previously, the equimolar BAPCs

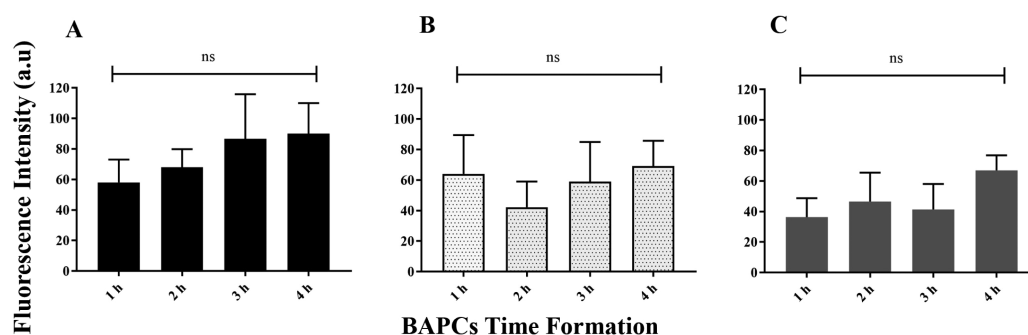


Figure 4. Time dependence at 4 °C for loading of Rhodamine 6G (100 μ M) for BAPCs prepared at different peptide ratios (1:0 panel A), 0.5:0.5 (panel B), and 0:1. (panel C). Data represent mean values + SEM of three experiments combined. Differences between values were compared by 2-way ANOVA using Bonferroni as post-test. Nonstatistical significance (ns) was considered when $p > 0.05$.

displayed predominantly random coil at 4 °C, mixed random and beta at 25 °C and beta at 37 °C. To better understand the effects of peptide ratio on structure in the assembled peptides, the secondary structures were analyzed by circular dichroism (CD).

This analysis was repeated for the five different ratios to examine the contributions of the two peptide sequences to the assembled structures. For these CD studies, 1 mM BAPCs were prepared using the five ratios used in Figure 3 assembled at 4, 25, and 37 °C for 75 min before recording the CD spectra at 25 °C (Figure 5). The BAPCs composed of 100% (Figure 5A) and 80% (Figure 5B) (Ac-FLIVI)₂-K-K₄-CO-NH₂ display mostly random coil secondary structure with a strong minimum at 198 nm at all three temperatures. The 100% (Ac-FLIVI)₂-K-K₄-CO-NH₂ BAPCs (Figure 5A) shows a minor minimum at 222 nm, suggesting a minor helical component. This structure is absent in the 80% (Ac-FLIVI)₂-K-K₄-CO-NH₂ BAPCs (Figure 5B). The equimolar ratio (Figure 5C) adopts the random coil conformation only at 4 °C. With increasing temperatures (25 and 37 °C) a mixture of random (198 nm) and beta structures (218 nm) are present. The 20% (Figure 5D) (Ac-FLIVI)₂-K-K₄-CO-NH₂ BAPCs show increasing amounts of beta with a decrease in random coil at elevated temperatures. The 0% (Figure 5E) (Ac-FLIVI)₂-K-K₄-CO-NH₂ BAPCs shows essentially only beta structure at all temperatures. Examining all of these data reveals that (Ac-FLIVI)₂-K-K₄-CO-NH₂ is unstructured while (Ac-FLIVIGSII)₂-K-K₄-CO-NH₂ adopts beta structure and that mixtures of the two peptides produce BAPCs with both structures present. A summary of this data is shown in Table S1 (Supporting Information). From previous studies²² only BAPCs showing mix conformations underwent fusion. Those prepared under conditions where random or beta structure predominated, were uniform and size stable 20–30 nm capsules that formed and remained as such when transitioned to higher temperatures.

A composite figure comparing the final spectra for the 4 °C annealing temperature is shown in Figure 6. This figure shows the relative contributions of the two sequences to the final structure of the peptides in the assembled BAPCs.

The BAPC bilayers composed of just unstructured peptides should show a decrease in thermal stability over those where beta-structure interpeptide hydrogen bonding predominates. Over the temperature range tested (up to 95 °C) there was no difference in stability (based on retention of the quenched Eosin Y). Hydrophobic interactions must be providing the cohesive forces that maintain their assembled structures to 95 °C. Perhaps at temperatures above the range we tested,

differences in thermal stability will become apparent. The π - π stacking interactions of the phenylalanines that populate the bilayer interface do not appear to be involved based on atomistic simulations previously reported.²⁸

The observation that all of these mixed and more homogeneous structures support assembly and temperature stability imply that these structural arrangements have to be stabilized in different ways. The extended random coil structures would have to form bilayers with a longer cross-sectional distance or as random coils they could have a shorter cross-sectional distance if they interdigitated. Analogously, the predominantly beta-sheet containing BAPCs should have the shortest cross-sectional distance. Differences in the thickness of the bilayer should affect the size of the BAPCs.

To test this hypothesis, BAPCs prepared at 4 °C (3 h) were analyzed at 25 °C by dynamic light scattering (DLS). Under these conditions the BAPCs form uniform stable structures, even when moved to the higher temperature. Three separate preparations were analyzed (Figure 7). This experiment clearly demonstrates that BAPCs prepared with different peptide ratios adopt different sizes to accommodate for aggregate differences in secondary structure. DLS experiments were conducted using 1 mM solutions of the peptides with the five (Ac-FLIVI)₂-K-K₄-CO-NH₂ to (Ac-FLIVIGSII)₂-K-K₄-CO-NH₂ ratios (1:0, 0.8:0.2, 0.5:0.5, 0.2:0.8, and 0:1). The average diameters (in nm) observed were 45.9 ± 4.7 , 42.2 ± 5.8 , 24.0 ± 2.8 , 19.5 ± 2.4 , and 11.2 ± 2.1 , respectively. The DLS value observed for the 0.5:0.5 ratio is in excellent agreement with those observed in our earlier TEM experiments.¹⁹ Prior to performing the experiments described herein, we hypothesized that the longer peptide sequence would yield larger BAPCs. Given the present findings the larger peptide's propensity to form compacted beta-structure prevails, thereby yielding the smallest structures.

Another interesting observation is that despite their size differences, equimolar batches of the different ratios encapsulate the same amount of dye. We observe less than nanomolar concentrations of free peptide by mass spectrometry after filtering BAPCs with a 30 kDa cutoff Amicon cellulose centrifugal filter (Merck). This results points to an extremely low critical association constant. Our best guess is that nearly all of the peptides participate in BAPC assembly or aggregation, with the pure (Ac-FLIVIGSII)₂-K-K₄-CO-NH₂ yielding a greater number of smaller BAPCs while the shorter (Ac-FLIVI)₂-K-K₄-CO-NH₂ forming fewer larger BAPCs while the peptides are in an extended conformation. To further investigate the biophysical properties of BAPCs, we analyzed the ZP for the five ratios analyzed by DLS (1:0, 0.8:0.2, 0.5:0.5,

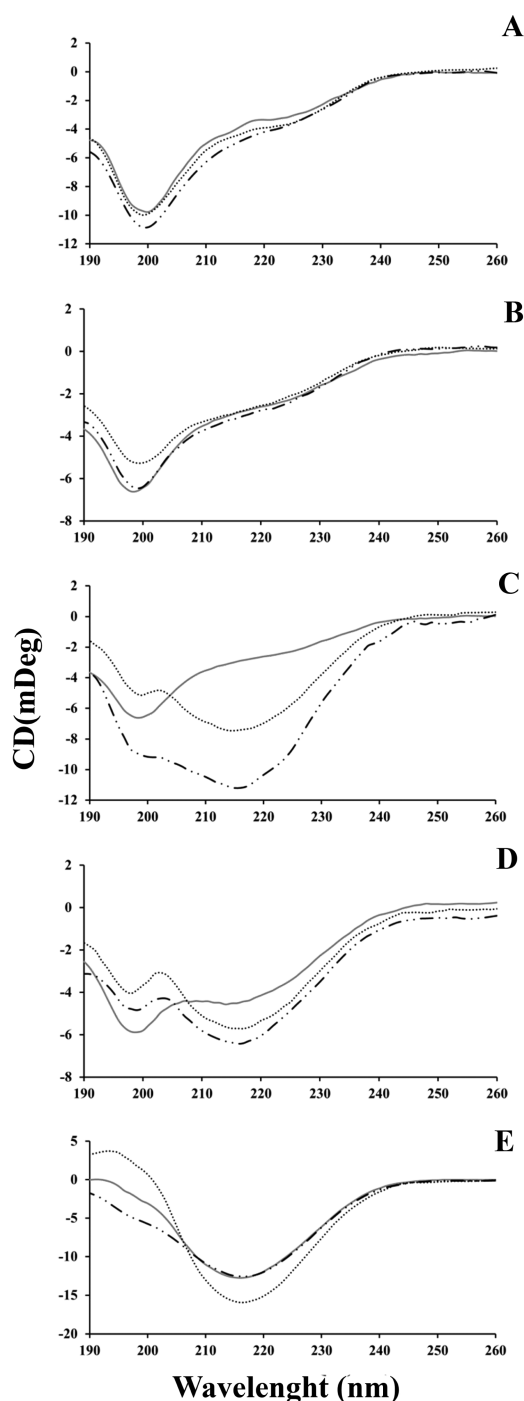


Figure 5. Circular dichroism spectra for five different ratios prepared at 4 °C (gray), 25 °C (dotted), or 37 °C (dot-dashed) for 75 min. All scans were performed at 25 °C. Panels A–E represent the ratios 0:1, 0.8:0.2, 0.5:0.5, 0.2:0.8, and 0:1 of (Ac-FLIVI)₂-K-K₄-CO-NH₂:(Ac-FLIVIGSII)₂-K-K₄-CO-NH₂, respectively.

0.2:0.8, and 0:1). The 1:0, 0.8:0.2, 0.2:0.8, and 0:1 ratios showed similar ZP's. The basis for the 0.5:0.5 ratio showing the higher ZP (~57 mV) is unclear. We hypothesized that this higher surface charge at this ratio affects assembly in the presence of Eosin Y leading to precipitation.

In Vitro Transfection Efficiency of BAPCS Assembled at Different Temperatures and with Different (Ac-FLIVI)₂-K-K₄-CO-NH₂:(Ac-FLIVIGSII)₂-K-K₄-CO-NH₂ Ratios. In a recent publication we demonstrated the ability of

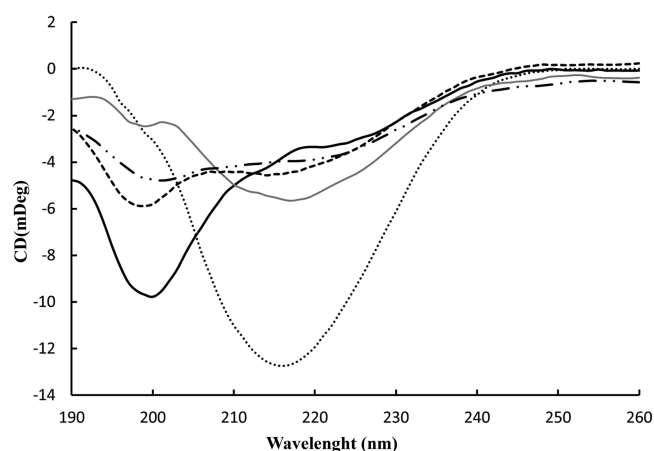


Figure 6. CD spectra of BAPCs composed of different ratios of (Ac-FLIVI)₂-K-K₄-CO-NH₂:(Ac-FLIVIGSII)₂-K-K₄-CO-NH₂ assembled at 4 °C. The spectra shown are 1:0 (dark solid line), 0.8:0.2 (dashed line), 0.5:0.5 (dot/dashed line), 0.2:0.8 (light gray line), and 0:1 (dotted line).

nanosized BAPCs to deliver plasmid DNA of different size into cells in culture.²¹ Transfection rates of ~55% were achieved with minimal cytotoxicity. The transfection protocol was optimized by testing different BAPCs concentrations and transfection buffers. Cells were also incubated with the BAPCs–DNA complexes for periods ranging from 2 to 12 h. Optimal transfection rates were obtained using BAPCs at 45 μM and 2.5 μg of DNA with an incubation period of 4–6 h in Opti-MEM I Reduced Serum Media.²¹ BAPCs were prepared using an equimolar concentration of (Ac-FLIVI)₂-K-K₄-CO-NH₂:(Ac-FLIVIGSII)₂-K-K₄-CO-NH₂. They were annealed at 25 °C and subsequently incubated at 4 °C for 1 h and then rewarmed to 25 °C, thereby fixing their size (20–30 nm). In this article, we analyzed how transfection efficiency was affected by preparing BAPCs at different temperatures and different peptide ratios. BAPCs were prepared with the following (Ac-FLIVI)₂-K-K₄-CO-NH₂:(Ac-FLIVIGSII)₂-K-K₄-CO-NH₂ ratios –1:0, 0.5:0.5, and 0:1. Also, capsules were annealed at 4, 25, and 37 °C.

HEK-293 cells were incubated with BAPCs associated with a 4.7 kb GFP-encoding plasmid and transfection efficiency was monitored qualitatively by fluorescence microscopy and quantified using fluorescence-activated cell sorting (FACS). Ghost Dye Red 780 was used to identify and then exclude dead cells from the analysis. Dead cells with compromised membranes allow Ghost Dye to permeate and bind amine groups of intracellular proteins resulting in fluorescence much brighter than live cells which are impermeant to Ghost Dye.²⁹ We selected this dye because the emission peak is 780 nm and do not overlap with the emission peak of GFP (509 nm), thus ensuring the exclusion of false positives. As shown in Figure 9A–D, the percent of dead cells is minimum for all the formulations tested (<1%), proving that BAPCs are extremely biocompatible. Maximal transfection rates were observed for BAPCs annealed at 4 and 37 °C using just (Ac-FLIVIGSII)₂-K-K₄-CO-NH₂ (0:1 ratio) (Figure 8A), and there was no significant difference between this ratio and the popular commercial transfection reagent (JetPRIME) (Figure 8A). For BAPCs prepared at 4 °C the size decreases from 46 to 25 to 10 nm (Figure 7A), and the transfection rate increases from ~39% to 41% to 70% (Figure 8B). Furthermore, BAPCs

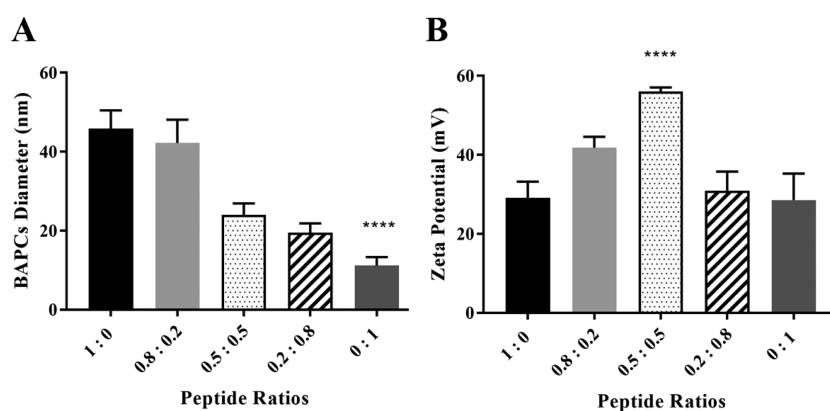


Figure 7. Average diameter (A) and zeta potential (B) of BAPCs formed at five different (Ac-FLIVI)₂-K-K₄-CO-NH₂:(Ac-FLIVIGSII)₂-K-K₄-CO-NH₂ ratios. BAPCs solutions (1 mM) were hydrated at 4 °C and scanned at 25 °C. Data represent mean values + SEM of three experiments combined. Differences between values were compared by 2-way ANOVA using Bonferroni as post-test. Statistical significance: (****)*p* < 0.0001, 0:1 vs 0.5:0.5 (A) and 0:1 vs 0.5:0.5 (B).

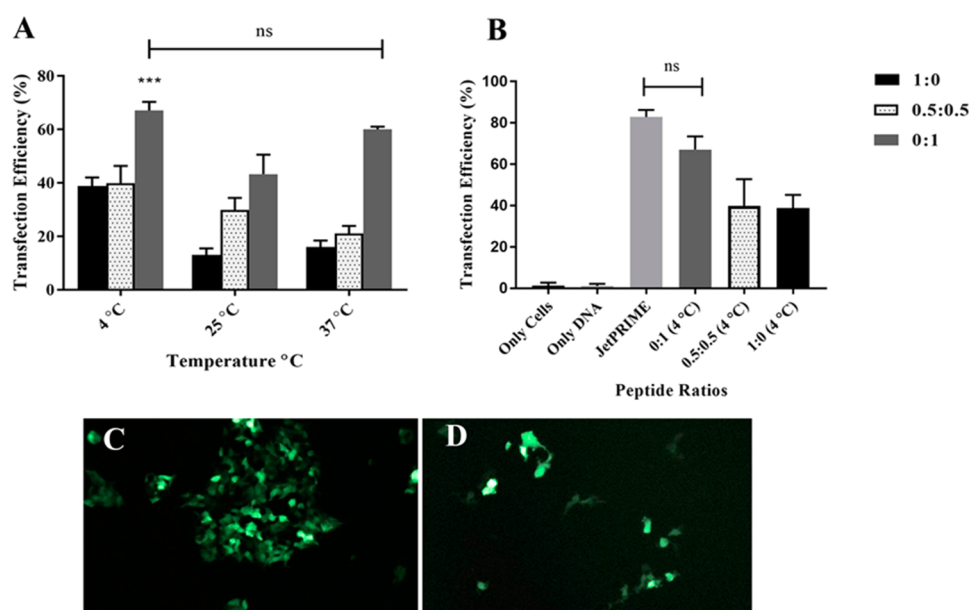


Figure 8. Transfection efficiency of BAPCs-DNA nanoparticles formed at different (Ac-FLIVI)₂-K-K₄-CO-NH₂:(Ac-FLIVIGSII)₂-K-K₄-CO-NH₂ ratios and annealed at different temperatures. HEK-293 cells transfected with BAPCs solutions hydrated at 4, 25, and 37 °C and subsequently mixed with 2.5 μg of GFP-encoding plasmid (A). HEK-293 transfected with BAPCs solutions hydrated only at 4 °C and subsequently mixed with 2.5 μg of GFP-encoding plasmid. Positive (JetPRIME) and negative (only DNA) controls were included. (B) Fluorescence microscope images of HEK-293 cells transfected only with (Ac-FLIVIGSII)₂-K-K₄-CO-NH₂ (C) and only with (Ac-FLIVI)₂-K-K₄-CO-NH₂ (D). Data represent mean values + SEM of three experiments combined. Differences between values were compared by 2-way ANOVA using Bonferroni as post-test. Statistical significance: (****)*p* < 0.0001, 0:1 vs 0.5:0.5 and 1:0. Nonstatistical significance (ns) was considered when *p* > 0.05.

annealed at 4 and 37 °C displayed beta-structure (Table 1S and Figure 5), suggesting that not only the size but also the secondary structure (beta-structure) are influencing transfection rates.

By exploring this alternative method to assemble BAPCs, we were able to enhance transfection efficiency ~15% (compared with our previous method) while maintaining low cytotoxicity as demonstrated with flow cytometry analysis.

CONCLUSIONS

Although our initial assumption has been that BAPC formation required both longer and shorter branched amphipathic peptides, the results presented above show that BAPCs can be prepared from either of the two peptides by themselves or mixtures thereof. The shorter peptide (FLIVI)₂-K-K₄-CO-NH₂

imparts random secondary structure to the BAPCs at each temperature. The larger peptide (FLIVIGSII)₂-K-K₄-CO-NH₂ folds, yielding beta-structure at all temperatures above 4 °C. Combining the peptides generates mixed secondary structures. All ratios resulted in thermally stable constructs. The results of this experiment show that we can now prepare stable, homogeneous BAPCs that can be made to incrementally vary in diameter from ~10 to 45 nm.

Many of our most current applications involve the delivery of dsDNA and dsRNA, which bind to the surface of preformed BAPCs. In this report we demonstrated that the ratio of the two peptides and the annealing temperatures affected the delivery efficiencies of DNA in HEK-293 cells. Previously, we reported that BAPCs (equimolar concentration) annealed at 25 °C and subsequently incubated at 4 °C for 1 h and then

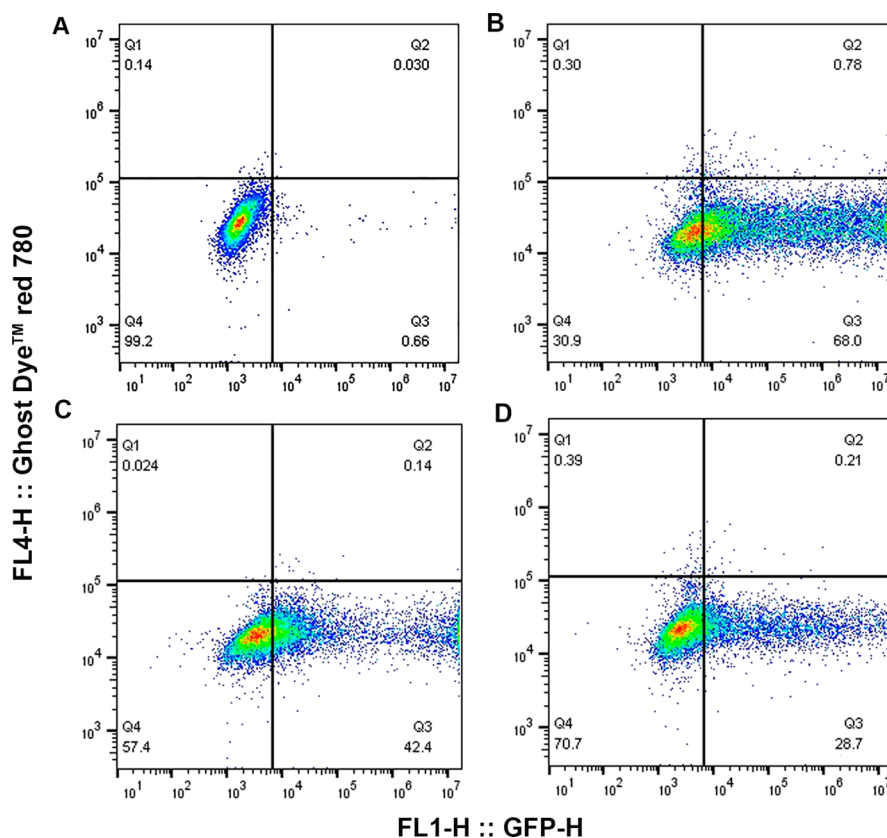


Figure 9. Flow cytometry analysis of GFP-expressing HEK-293 cells after 48 h post-transfection with only cells (A) 1:0, (B) 1:1 (C), and 0:1 (D). BAPCs were hydrated at 4 °C; HEK-293 cells were incubated with the nanoparticles for 4 h in reduced serum media and 1 mM CaCl₂.

rewarmed to 25 °C achieved transfection rates of ~55%. Higher transfection rates were observed in this experiments. BAPCs annealed at 4 and 37 °C using just (Ac-FLIVIGSII)₂-K-K₄-CO-NH₂ (0:1 ratio) displayed efficiencies approaching 70%. It is noteworthy that those annealing temperatures (4 and 37 °C) generated beta secondary structure. The ratio (0:1) generated BAPCs with sizes ~10 nm and ZP (~25 mV). Overall, these results suggested that those parameters are critical factors influencing the BAPCs' ability to deliver nucleic acids into cells. Further studies will consist in studying the morphologies of the BAPCs–DNA complexes that generated the highest delivery rates.

■ ASSOCIATED CONTENT

● Supporting Information

The Supporting Information is available free of charge on the ACS Publications website at DOI: 10.1021/acs.langmuir.7b00912.

Fluorescence scans of Rhodamine 6G at different concentrations (Figure 1S) and a summary of the secondary structures for BAPCs prepared at different ratios and temperatures (Figure 2S) (PDF)

■ AUTHOR INFORMATION

Corresponding Author

*E-mail jtomich@ksu.edu (J.M.T.).

ORCID

John M. Tomich: 0000-0001-7848-8307

Author Contributions

S.d.M.B. and L.A.A. made equal contributions.

Notes

The authors declare no competing financial interest.

■ ACKNOWLEDGMENTS

This publication is contribution number 16-376-J from the Kansas Agricultural Experiment Station. Partial support for this project was provided by the Terry Johnson Cancer Center at Kansas State University (Innovation Award to J.M.T. and summer graduate research support to S.K.W). L.A.A. acknowledges financial support from Auburn University Cellular and Molecular Biosciences Peaks of Excellence Program. The scholarship award to S.B. was provided by the Coordenação de Aperfeiçoamento de Pessoal de Nível Superior (CAPES) Process number PDSE-99999.007690/2014-02; Affiliation: CAPES Foundation, Ministry of Education, Brasília, DF, Brazil. We thank Prof. Allan E. David (Samuel Ginn College of Engineering, Auburn University) for his contribution on the ZP assays.

■ REFERENCES

- (1) Discher, D. E.; Eisenberg, A. Polymer vesicles. *Science* **2002**, *297*, 967–973.
- (2) Bellomo, E. G.; Wyrsta, M. D.; Pakstis, L.; Pochan, D. J.; Deming, T. J. Stimuli-responsive polypeptide vesicles by conformation-specific assembly. *Nat. Mater.* **2004**, *3*, 244–248.
- (3) Holowka, E. P.; Pochan, D. J.; Deming, T. J. Charged polypeptide vesicles with controllable diameter. *J. Am. Chem. Soc.* **2005**, *127*, 12423–12428.
- (4) Kabanov, A. V.; Batrakova, E. V.; Alakhov, V. Y. Pluronic block copolymers as novel polymer therapeutics for drug and gene delivery. *J. Controlled Release* **2002**, *82*, 189–212.

- (5) Ghosh, S.; Reches, M.; Gazit, E.; Verma, S. Bioinspired design of nanocages by self-assembling triskelion peptide elements. *Angew. Chem., Int. Ed.* **2007**, *46*, 2002–2004.
- (6) Akter, N.; Radiman, S.; Mohamed, F.; Reza, M. I. Self-assembled potential bionanocarriers for drug delivery. *Mini-Rev. Med. Chem.* **2013**, *13*, 1327–39.
- (7) Fletcher, J. M.; Harniman, R. L.; Barnes, F. R.H.; Boyle, A. L.; Collins, A.; Mantell, J.; et al. Self-Assembling Cages from Coiled-Coil Peptide Modules. *Science* **2013**, *340*, 595–599.
- (8) Vauthey, S.; Santoso, S.; Gong, H.; Watson, N.; Zhang, S. Molecular self-assembly of surfactant-like peptides to form nanotubes and nanovesicles. *Proc. Natl. Acad. Sci. U. S. A.* **2002**, *99*, 5355–5360.
- (9) Matsuura, K.; Murasato, K.; Kimizuka, N. Artificial peptide-nanospheres self-assembled from three-way junctions of β -sheet-forming peptides. *J. Am. Chem. Soc.* **2005**, *127*, 10148–10149.
- (10) Matsuura, K.; Watanabe, K.; Sakurai, K.; Matsuzaki, T.; Kimizuka, N. Self-assembled synthetic viral capsids from a 24-mer viral peptide fragment. *Angew. Chem., Int. Ed.* **2010**, *49*, 9662–9665.
- (11) Van Hell, A. J.; Costa, C. I.; Flesch, F. M.; Sutter, M.; Jiskoot, W.; Crommelin, D. J. A.; Hennink, W. E.; Mastrobattista, E. Self-assembly of recombinant amphiphilic oligopeptides into vesicles. *Biomacromolecules* **2007**, *8*, 2753–2761.
- (12) Reches, M.; Gazit, E. Formation of Closed-Cage Nanostructures by Self-Assembly of Aromatic Dipeptides. *Nano Lett.* **2004**, *4*, 581–585.
- (13) Mishra, A.; Panda, J. J.; Basu, A.; Chauhan, V. S. Nanovesicles Based on Self-Assembly of Conformationally Constrained Aromatic Residue Containing Amphiphilic Dipeptides. *Langmuir* **2008**, *24*, 4571–4576.
- (14) Naskar, J.; Roy, S.; Joardar, A.; Das, S.; Banerjee, A. Self-assembling dipeptide-based nontoxic vesicles as carriers for drugs and other biologically important molecules. *Org. Biomol. Chem.* **2011**, *9*, 6610–6615.
- (15) Koley, P.; Pramanik, A. Multilayer vesicles, tubes, various porous structures and organo gels through the solvent-assisted self-assembly of two modified tripeptides and their different applications. *Soft Matter* **2012**, *8*, 5364–5374.
- (16) Barros, S. M.; Whitaker, S. K.; Sukthankar, P. R.; Gudlur, S.; Warner, M.; Beltrão, E. I. C.; Tomich, J. M. A Review of Solute Encapsulating Nanoparticles used as Delivery Systems with Emphasis on Branched Amphipathic Peptide Capsules. *Arch. Biochem. Biophys.* **2016**, *596*, 22–42.
- (17) Sukthankar, P.; Gudlur, S.; Avila, L. A.; Whitaker, S.; Katz, B. B.; Hiromasa, Y.; Gao, J.; Thapa, P.; Moore, D.; Iwamoto, T.; Tomich, J. M. Branched Oligopeptides Form Nano-Capsules with Lipid Vesicle Characteristics. *Langmuir* **2013**, *29*, 14648–14654.
- (18) Sukthankar, P.; Whitaker, S. K.; Garcia, M.; Herrera, A.; Boatwright, M.; Prakash, O.; Tomich, J. M. Thermally induced conformational transitions in nascent branched amphiphilic peptide capsules. *Langmuir* **2015**, *31*, 2946–2955.
- (19) Yan, X.; He, Q.; Wang, K.; Duan, L.; Cui, Y.; Li, J. Transition of Cationic Dipeptide Nanotubes into Vesicles and Oligonucleotide Delivery. *Angew. Chem.* **2007**, *119*, 2483–2486.
- (20) Avila, L. A.; Aps, L. R. M. M.; Sukthankar, P.; Ploscariu, N.; Gudlur, G.; Šimo, L.; Szoszkiewicz, R.; Park, Y.; Lee, S. W.; Iwamoto, T.; Ferreira, L.; Tomich, J. M. Alternate supramolecular structures for different ratios of branched amphiphilic cationic peptide /DNA assemblies: Correlation with gene delivery. *Mol. Pharmaceutics* **2015**, *12*, 706–715.
- (21) Avila, L. A.; Aps, L. M. M.; Ploscariu, N.; Sukthankar, P.; Guo, R.; Wilkinson, K. E.; Games, P.; Szoszkiewicz, R.; Alves, R. P. S.; Diniz, M. O.; Fang, Y.; Ferreira, L. C. S.; Tomich, J. M. Gene delivery and immunomodulatory effects of plasmid DNA associated with Branched Amphiphilic Peptide Capsules. *J. Controlled Release* **2016**, *241*, 15–24.
- (22) Kempe, M.; Barany, G. CLEAR: A Novel Family of Highly Cross-Linked Polymeric Supports for Solid Phase Synthesis. *J. Am. Chem. Soc.* **1996**, *118*, 7083–7093.
- (23) Tomich, J. M.; Wallace, D. P.; Henderson, K.; Brandt, R.; Ambler, C. A.; Scott, A. J.; Mitchell, K. E.; Radke, G.; Grantham, J. J.; Sullivan, L. P.; Iwamoto, T. Aqueous solubilization of transmembrane peptide sequences with retention of membrane insertion and function. *Biophys. J.* **1998**, *74*, 256–267.
- (24) Chen, R. F. Measurements of absolute values in biochemical fluorescence spectroscopy. *J. Res. Natl. Bur. Stand., Sect. A* **1972**, *76*, 593–606.
- (25) Sponer, H. Remarks on the Absorption Spectra of Phenylalanine and Tyrosine in Connection with the Absorption in Toluene and Paracresol. *J. Chem. Phys.* **1942**, *10*, 672.
- (26) Savitzky, A.; Golay, M. J. E. Smoothing and Differentiation of Data by Simplified Least Squares Procedures. *Anal. Chem.* **1964**, *36*, 1627–1639.
- (27) Gorry, P. A. General least-squares smoothing and differentiation by the convolution (Savitzky-Golay) method. *Anal. Chem.* **1990**, *62*, 570–573.
- (28) Jia, Z.; Whitaker, S. K.; Tomich, J. M.; Chen, J. Organization and Structure of Branched Amphipathic Oligopeptide Bilayers. *Langmuir* **2016**, *32*, 9883–9891.
- (29) Kaushik, G.; Venugopal, A.; Ramamoorthy, P.; Standing, D.; Subramaniam, D.; Umar, S.; Jensen, R.; Anant, s.; Mammen, J. M. V. Honokiol inhibits melanoma stem cells by targeting notch signaling. *Mol. Carcinog.* **2015**, *54*, 1710–1721.